Journal of Chromatography A, 1218 (2011) 5794–5800

Contents lists available at ScienceDirect

Journal of Chromatography A

journal homepage: www.elsevier.com/locate/chroma

Injection profiles in liquid chromatography II: Predicting accurate injection-profiles for computer-assisted preparative optimizations

Patrik Forssén[a], Lena Edström[b], Jörgen Samuelsson[a], Torgny Fornstedt[a,b,*]

[a] Department of Chemistry and Biomedical Sciences, Karlstad University, SE-651 88 Karlstad, Sweden
[b] Department of Physical and Analytical Chemistry, BMC Box 599, SE-751 24 Uppsala, Sweden

ARTICLE INFO

Article history:
Received 14 January 2011
Received in revised form 17 May 2011
Accepted 9 June 2011
Available online 22 June 2011

Keywords:
Injection profile
Preparative chromatography
Exponentially modified Gaussian
Modeling
Simulation
Optimization

ABSTRACT

In computer assisted optimization of liquid chromatography it has been known for some years that it is important to use experimental injection profiles, instead of rectangular ones, in order to calculate accurate elution bands. However, the incorrectly assumed rectangular profiles are still mostly used especially in numerical optimizations. The reason is that the acquisition of injection profiles, for each injection volume and each flow rate considered in a computer-assisted optimization requires a too large number of experiments. In this article a new function is proposed, which enables highly accurate predictions of the injection profiles and thus more accurate computer optimizations, with a minimum experimental effort. To model the injection profiles for any injection volume at a constant flow rate, as few as two experimental injection profiles are required. If it is desirable to also take the effect of flow rate on the injection profiles into account, then just two additional experiments are required. The overlap between fitted and experimental injection profiles at different flow rates and different injection volumes were excellent, more than 90%, using experimental injection profiles from just four different injection volumes at two different flow rates. Moreover, it was demonstrated that the flow rate has a minor influence on the injection profiles and that the injection volume is the main parameter that needs to be accounted for.

1. Introduction

Preparative liquid chromatography is an important technique for large-scale isolation and purification of high-value compounds after prior unit operations. To be able to numerically optimize the process, several system parameters are required to be known, *e.g.* adsorption isotherm, column model, and injection profile. In this study the focus will be on injection profiles.

In our preceding fundamental study it was observed that the injection profile becomes more eroded with increased: (i) flow rate, (ii) viscosity of the eluent, (iii) injection volume, (iv) the inner diameter of the injection-loop tubing and (v) size of the solute [1]. In that study, a 2D-convection-diffusion differential equation with cylindrical coordinates taking radial diffusion and parabolic flow profiles into account was used to describe the appearance of the experimental injection profiles. However, it is hard/impossible to model all dead volume contributions, and therefore the model is mainly suited to gain qualitative understanding of the overall mechanisms that contribute to the dispersion of the injection profile. In process optimization, several system parameters, that are generally varied, will affect the injection profile, *i.e.* flow rate, injection volume, and eluent composition. For a more accurate process optimization than the 2D-model can provide, it is crucial to properly account for the effect of these parameters on the injection profiles using a more pragmatic modeling approach.

In process optimization, elution profiles for different conditions are calculated [2]. This is done by solving the partial differential column model, which requires injection profiles as boundary conditions. Often simple rectangular injection profiles are used [2–5], even though the true injection profile generally deviates strongly from the rectangular pulse [1,6,7]. It is now widely acknowledged that simulation of elution profiles using experimental, or models that mimic experimental injection profiles, gives a better agreement with experimental data as compared to when a rectangular injection profile is used [8–10]. To improve the agreement, several approaches have been used to imitate the true injection profile, *e.g.* using one half Gaussian [10], quasi-Gaussian (two half Gaussian with different standard deviations) [11], and exponentially modified Gaussian (EMG, a convolution of Gaussian and an exponential decay function) functions [12]. In the case of large injection volumes, the injection profiles can reach a concentration plateau and none of the previous stated

* Corresponding author at: Department of Chemistry and Biomedical Sciences, Karlstad University, SE-651 88 Karlstad, Sweden. Tel.: +46 54 700 19 60.
E-mail address: Torgny.Fornstedt@kau.se (T. Fornstedt).

0021-9673/$ – see front matter © 2011 Elsevier B.V. All rights reserved.
doi:10.1016/j.chroma.2011.06.063

models are able to model this. Felinger et al. modeled large pump pulses by using the convolution of the EMG function and a rectangular pulse [12]. Fitting of different empirical functions to elution profiles, spectroscopic data and flow injection analysis have been carried out for a long time [13]. The reason for doing such analyses has been to: reduce the signal-to-noise ratio, deconvolute partially resolved peaks, determinate peak properties such as moments, etc. [13]. Mainly the EMG and the Gaussian, and to a lesser extent also the Edgeworth/Cramér, Giddings, Gram/Charlier, Log-normal, Poisson and Weibull, functions have been used [13].

The studies described above [6–12] are not focused on the injection profile appearance *per se*, and the experiments are performed with a fixed flow rate and/or fixed injection volume. The aim of this study was to develop a relationship that can be used to rapidly and correctly model the injection profiles under various different operational conditions, which is necessary for a more accurate prediction using computer-assisted optimization. A pragmatic "soft" modeling approach will be used, *i.e.* the goal is only to derive a closed, easily evaluated, function that can describe the injection profiles. The function is not intended to describe the actual physiochemical processes and the function parameters are not required to have any physical interpretation. To achieve this, convolution of functions is used to describe the injection profiles when the flow rates and injection volumes varies.

In particular, different numerical approaches, for describing injection profiles at different flow rates and injection volumes, are investigated. First a pragmatic approach is used that is based on interpolation of experimental injection profiles. Then a new fitting function is used that is determined using a much smaller set of experiential injection profiles. The overall goal is to reduce the required amount of experimentally determined injection profiles to a minimum, and still conduct highly accurate process optimization.

2. Theory

In this section, a function will be derived that can be used to model injection profiles that have "cut-off" peaks. It is a modification of the EMG function that is a convolution between a Gaussian pulse and an exponentially decaying function, this strategy is similar to the one used in [12]. The convolution between to functions, f and g, can be written as,

$$h(t) = (f * g)(t) = \int_{-\infty}^{\infty} f(s)g(2t - s)ds. \tag{1}$$

Notice that a slightly modified definition is used for technical reasons; usually the integrand $f(s) \times g(t - s)$ is used.

A Gaussian peak can be written,

$$f(t) = \frac{A}{\sigma\sqrt{2\pi}} \exp\left(-\frac{(t - t_0)^2}{2\sigma^2}\right), \tag{2a}$$

where A is the peak area, σ the standard deviation (peak width) and t_0 the peak position in time (mean of the Gaussian distribution). The function will be convolved with an exponentially decaying pulse that has an initial constant part,

$$g(t) = \begin{cases} 0 & , \quad t < (1 - \theta)t_0, \\ 1 & , \quad (1 - \theta)t_0 \le t < (1 + \theta)t_0, \\ \exp\left(\dfrac{-t + (1 + \theta)t_0}{\tau}\right) & , \quad t \ge (1 + \theta)t_0, \end{cases} \tag{2b}$$

here θ indicates the width of the constant part and τ is the decay speed of the exponential part, see Fig. 1. Eqs. (2a) and (2b) can be convolved using Eq. (1) and the result can be written in closed form as,

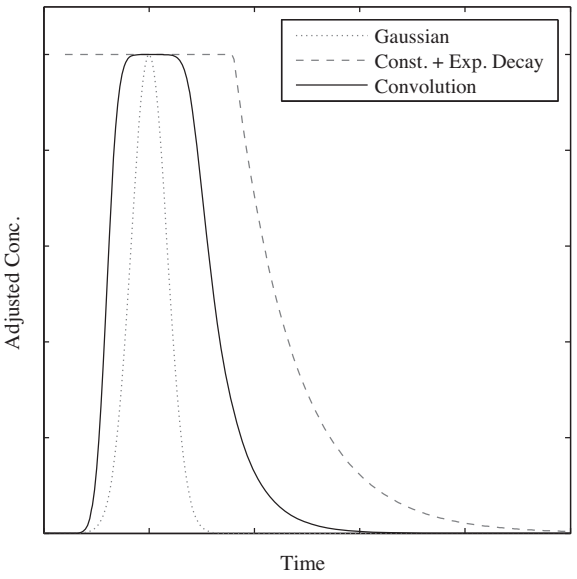

Fig. 1. Illustration of the convolution (solid) between a Gaussian pulse (dotted) and a pulse with a constant part and exponential decay (dashed).

$$h(t) = \frac{A}{2}\left[\operatorname{erf}\left(\frac{2t_0 - 2t + \theta}{\sqrt{2}\sigma}\right) + \operatorname{erf}\left(\frac{2t_0 + 2t + \theta}{\sqrt{2}\sigma}\right)\right] + \frac{A}{2}\exp\left(\frac{-2t + 2t_0 + \theta}{\tau} + \frac{\sigma^2}{2\tau^2}\right)\operatorname{erfc}\left(\frac{\sigma^2 - 2t\tau + 2t_0\tau + \tau\theta}{\sqrt{2}\sigma\tau}\right), \tag{3a}$$

where erf and erfc is the error function and complementary error function respectively, see Fig. 1. Notice that great caution must be taken during evaluation of the function h using floating point arithmetic! The term $\exp(\ldots) \times \operatorname{erfc}(\ldots)$ will result in problems with floating point accuracy of the type $\infty \times 0$ and the result will be erroneous. To avoid this Eq. (3a) can be rewritten as,

$$h(t) = \frac{A}{2}\left[\operatorname{erf}\left(\frac{2t_0 - 2t + \theta}{\sqrt{2}\sigma}\right) + \operatorname{erf}\left(\frac{2t_0 + 2t + \theta}{\sqrt{2}\sigma}\right)\right] + \frac{A}{2}\exp\left[\left(\frac{-2t + 2t_0 + \theta}{\tau} + \frac{\sigma^2}{2\tau^2}\right) + \ln\left(\operatorname{erfc}\left(\frac{\sigma^2 - 2t\tau + 2t_0\tau + \tau\theta}{\sqrt{2}\sigma\tau}\right)\right)\right]. \tag{3b}$$

However, this will instead result in problems with floating point underflow in the term $\ln(\operatorname{erfc}(\ldots))$. To avoid this, a special function $\ln \operatorname{erfc}(\ldots)$ is used to calculate this term, this function is defined as,

$$\ln\ \operatorname{erfc}(x) = \begin{cases} \ln(\operatorname{erfc}(x)), & x \le \bar{x}, \\ p_2(x - \bar{x})^2 + p_1(x - \bar{x}) + \ln(\operatorname{erfc}(\bar{x})), & x > \bar{x}, \end{cases} \tag{4}$$

where $\bar{x}$ is a threshold above which problems with underflow occurs and p_2, p_1 are constants that can be estimated by a least squares fit of $p_2(x - \bar{x})^2 + p_1(x - \bar{x}) + \ln(\operatorname{erfc}(\bar{x}))$ to values of $\ln(\operatorname{erfc}(x))$ for $x \le \bar{x}$, *i.e.*, here $\bar{x} = 26.5$, $p_2 = -0.99433$ and $p_1 = -52.95443$ are used.

3. Experimental

3.1. Apparatus

The experiments were performed on an Agilent 1100 and an Agilent 1200 system, both with the same experimental setup, consisting of a binary pump, an auto-sampler and a Diode Array UV detector equipped with an Agilent micro flow cell (Palo Alto, CA, USA). The loop volume was 900 μL (coiled sample loop) and injection volumes below 900 μL were performed with partial filling technique.

3.2. Chemicals

De-ionized water (conductivity 18.2 MΩ cm) for preparation of eluents was delivered from a ZMQS 5000Y Milli-Q Academic water purification system from Millipore (Molsheim, France). The organic modifier was methanol (CHROMASOLV quality) and the solute was 3-phenyl-1-propanol (PP, 98%).

3.3. Procedures

Samples of 1.0 mM PP dissolved in the eluent were used, except in the concentration dependence experiments. Injection profiles were measured at seven different injection volumes (5.0, 10.0, 25.0, 50.0, 100.0, 200.0 and 400.0 μL) at five different flow rates (0.25, 0.50, 1.0, 2.0, 3.0 mL/min) using 45/55 (v/v) MeOH/MilliQ water as eluent. One flow rate (2.0 mL/min) was complemented with equidistant injection volumes (25 μL steps) across the mentioned volume range, and additional volumes in the low range, 22 volumes in total. The volumes used were 5.0, 10.0, 15.0, 20.0, 25.0, 30.0, 40.0, 50.0, 75.0, 100.0, 125.0, 150.0, 175.0, 200.0, 225.0, 250.0, 275.0, 300.0, 325.0, 350.0, 375.0 and 400.0 μL. The concentration dependence was examined with 10.0 and 900.0 μL injections with concentrations of 1.0, 2.0, 3.0, 5.0, 10.0, 20.0, 30.0, 50.0, 100.0, 200.0, 300.0 and 400.0 mM, at the flow rates 0.50 and 3.0 mL/min The injection profiles were determined by connecting the auto-sampler directly to the detector cell by using the capillaries and pre-column filter normally used, but without the column. The influence of these connectors and dead-volumes on the shape of the injection profile was studied in a preceding paper [1]. The backpressure was regulated by application of a 0.17 μm I.D. capillary after the detector cell, generating around 15–20 bar backpressure. Also, a sufficient amount of available capillaries was connected between the pump and injector to keep the backpressure at around 60 bar (59–64) over the whole range of flows used in the injection profile part. Injection profiles were determined at 260 nm.

One must point out that the experimentally determined injection-profiles will differ some from the true injection profiles entering the top of the column. To reduce this deviation we have used low volume detector cells and low volume peek tubing's. In addition, a back pressure was placed after the detector to "emulate" a column to avoid potential pressure "artifacts". Because we use a low volume detector cell, its contribution to the total variance of the injection profile could be expected to be small, especially for larger injection volumes that are generally used in preparative applications.

4. Results and discussion

As a reference data set, a large number of measured experimental injection profiles are used. Notice that by using linear interpolation it is possible to estimate the injection profiles for intermediate injection volumes and flow rates from this data set. An example of interpolated injection profiles for a fixed flow rate can be seen in Fig. 2. The interpolation procedure means that fewer

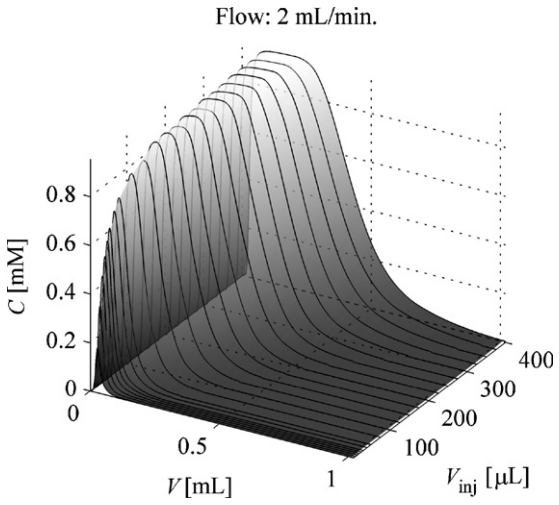

Fig. 2. Example of interpolation of injection profiles for injection volumes between 5.0 and 400.0 μL at the flow rate 2.0 mL/min. The experimental injection profiles are indicated by solid lines and the gray shaded area between the lines represents the interpolation. For a detailed report of the volumes used, see Section 3.3.

experimental injection profiles, than one for each experimental case, are required. However, to get acceptable agreement between experimental and interpolated injection profiles, a large number of experimental injection profiles are still required.

In the following text the eluted volume, V is used, instead of time, t, and also use the parameter V_0 instead of t_0, *i.e.*, Eq. (3b) is rewritten to,

$$C_{\text{fit}}(V) = \frac{A}{2}\left[\text{erf}\left(\frac{2V_0 - 2V + \theta}{\sqrt{2}\sigma}\right) + \text{erf}\left(\frac{2V_0 + 2V + \theta}{\sqrt{2}\sigma}\right)\right] + \frac{A}{2}\ \exp\left[\left(\frac{-2V + 2V_0 + \theta}{\tau} + \frac{\sigma^2}{2\tau^2}\right) + \ln\ \text{erfc}\left(\frac{\sigma^2 - 2V\tau + 2V_0\tau + \tau\theta}{\sqrt{2}\sigma\tau}\right)\right], \quad (5)$$

to describe injection profiles. Fitting experimental injection profiles to Eq. (5) will hopefully reduce the required amount of injection profiles even further.

4.1. The effect of injection parameters on the injection profiles

The parameters that might affect the shape of the injection profile when using the same substance and system setup are: (i) the sample concentration, (ii) the flow rate and (iii) the injection volume was examined. In Fig. 3a, the flow rate and injection volume was kept constant and the sample concentration was varied. As can be seen on the shape of the injection profiles it is almost identical, in other words the sample concentration is in this case not important to consider. In Fig. 3b, the injection volume and sample concentration was kept constant and the flow rate was varied. As can be seen, a slight shift of the profiles occurs with increasing flow rate, which is in accordance with our previous findings [1]. In Fig. 3c, the sample concentration and flow rate was kept constant and the injection volume was varied. As can be seen, there is a significant change in the profile shape when the injection volume changes; thus, this is the main parameter to consider.

4.2. Parameterization of injection profiles with varying injection volume

As was seen in the previous section, the injection volume is the major parameter that affects the shape of the injection profiles.

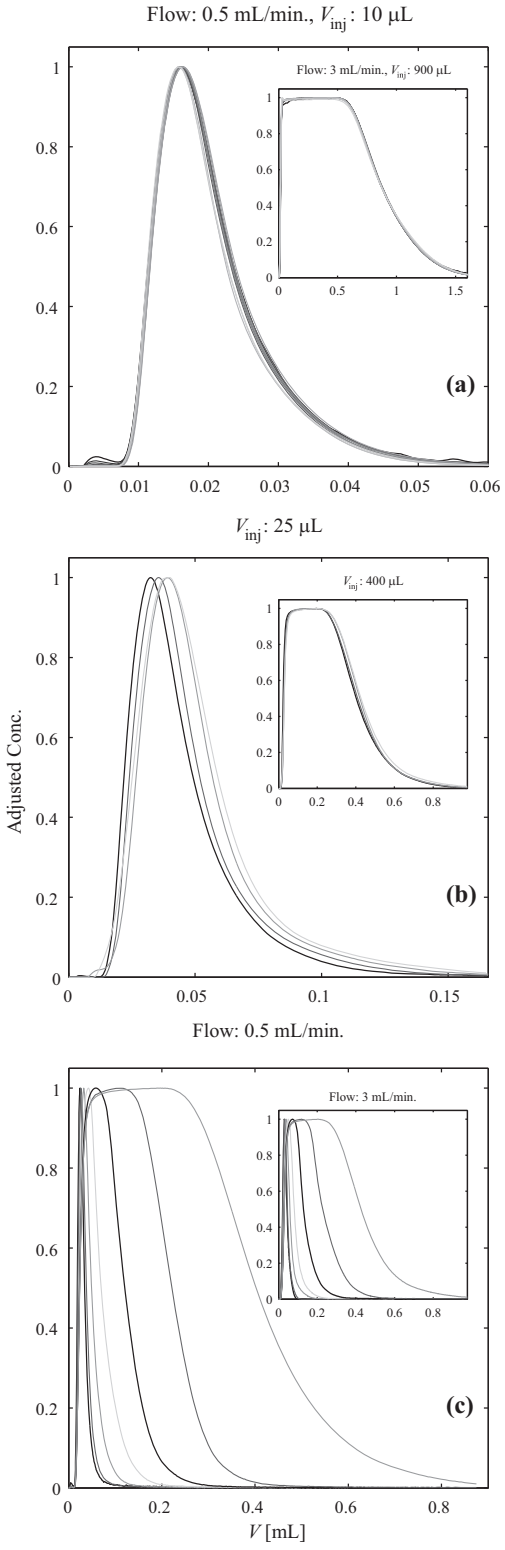

Fig. 3. The effect of injection parameters on the injection profiles, all data are adjusted to a peak height of 1. (a) Effect of varying the concentration: injection of 10.0 (main figure) or 900.0 µL (inset) of samples with concentration 1.0, 2.0, 3.0, 5.0, 10.0, 20.0, 30.0, 50.0, 100.0, 200.0, 300.0, 400.0 mM (darker lines corresponds to lower concentration) at the flow rate 0.50 (main figure) or 3.0 mL/min (inset). (b) Effect of varying the flow rate: injection of 25.0 (main figure) or 400.0 µL (inset) of a sample with concentration 1.0 mM at flow rates 0.25, 0.50, 1.0, 2.0, 3.0 mL/min (darker lines corresponds to lower flow rate). (c) Effect of varying the injection volume: injection of 5.0, 10.0, 25.0, 50.0, 100.0, 200.0, 400.0 µL (darker lines corresponds to lower injection volumes) of a sample with concentration 1.0 mM at flow rate 0.50 mL/min (main figure) or 3.0 mL/min (inset).

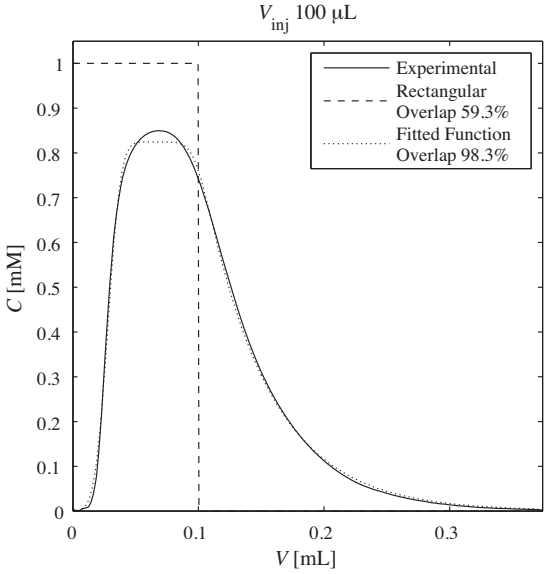

Fig. 4. Experimental injection profile (solid line), rectangular injection profile (dashed line) and fitted profile using Eq. (5) (dotted line), for a 100.0 µL injection at the flow rate of 2.0 mL/min. The overlap with the experimental profile was 59.3% for the rectangular injection profile and 98.3% for the profile fitted to Eq. (5).

This parameter is also the one that is varied in most practical situations, *e.g.* when using the inverse method to determine adsorption isotherm parameters [14] and in process optimization. Therefore we initially used a least squares procedure to fit Eq. (5) to experimental injection profiles with varying injection volumes while keeping the sample concentration fixed at 1.0 mM and the flow rate fixed at 2.0 mL/min. A fit to an experimental profile is shown in Fig. 4, together with the traditionally used rectangular injection profile. To quantify the overlap of experimental and fitted injection profiles, the total area overlap formula was used,

$$\text{Overlap} = 100\frac{\int_0^\infty \min_V(C_{\text{fit}}(V), C_{\text{exp}}(V))dV}{\int_0^\infty C_{\text{fit}}(V)dV}. \quad (6)$$

This formula calculates how much area that is shared by two 2D-objects with equal area, *i.e.*, how large percentage of each object area that is in the overlapping region. An overlap approaching 100% indicates complete overlap, while 0% indicates that they are completely separated. The degree of overlap between the experimental profile and the fitted profile in Fig. 4 is excellent (98.3%) compared to rectangular injection profile (59.3%).

Next, it was studied how the estimated parameters of the fitted function in Eq. (5) vary with different injection volumes. In Fig. 5, it is obvious that the parameters V_0 (Fig. 5a), V_{inj}/σ (Fig. 5b), τ (Fig. 5c) and θ (Fig. 5d) has a linear relationship with the injection volume V_{inj}. These linear relationships can be written,

$$\begin{aligned} &V_0(V_{\text{inj}}) \approx k_{V_0}V_{\text{inj}} + l_{V_0}, \\ &(V_{\text{inj}}/\sigma)(V_{\text{inj}}) \approx k_\sigma V_{\text{inj}} + l_\sigma \Leftrightarrow \sigma(V_{\text{inj}}) = \frac{V_{\text{inj}}}{k_\sigma V_{\text{inj}} + l_\sigma}, \\ &\tau(V_{\text{inj}}) \approx k_\tau V_{\text{inj}} + l_\tau, \\ &\theta(V_{\text{inj}}) \approx k_\tau V_{\text{inj}} + l_\tau, \end{aligned} \quad (7)$$

where k_* and l_* are constants estimated by fitting a straight line to the data points in Fig. 5 using a linear least squares procedure. Notice that the variation of the area parameter A in Eq. (5) is of no interest, because it reflects the area under the peak and it is equal to the injected amount of substance.

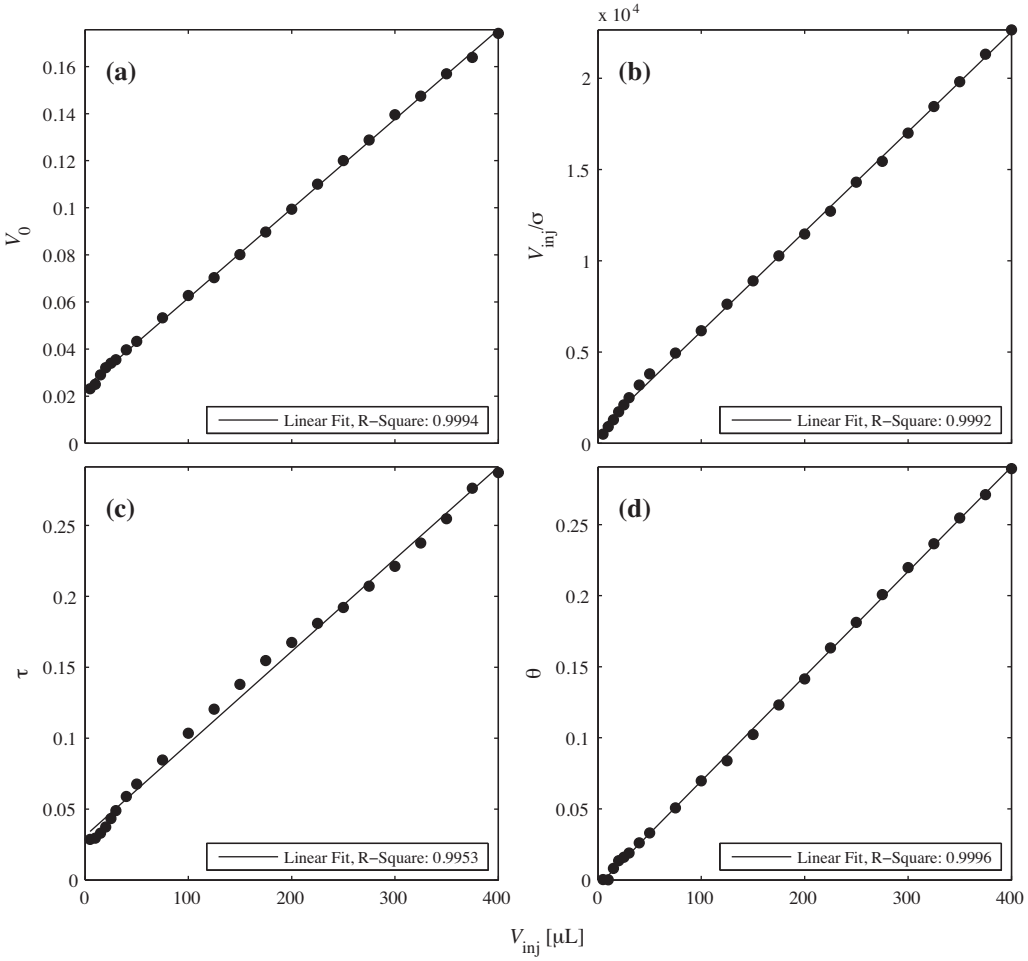

Fig. 5. Illustration of how the parameters (a) V_0, (b) V_{inj}/σ, (c) τ and (d) θ (symbols) in Eq. (5) changes when the injection volume V_{inj} is varied. The parameters are estimated from least squares fitting to experimental injection profiles and the solid line is a linear least square fit to the parameters where the *R*-square value was 0.9994 in (a), 0.9992 in (b), 0.9953 in (c) and 0.9996 in (d).

This means that the minimum requirement, to be able to estimate the injection profiles for any injection volume by using Eqs. (5) and (7), is merely two different injection volumes. However, in practice it is recommended to use more than two experimental injection profiles to be able to estimate the constants k_* and l_* in Eq. (7) accurately.

4.3. Parameterization of injection profiles with varying injection volume and flow

As can be seen in Fig. 3b, the flow rate affects the shape of the injection profiles to a lesser extent than the injection volume. In most practical applications the flow rate is kept constant, why there usually is no need to take this into account. Even for applications when the flow rate does vary, estimating the injection profiles for one flow rate in the middle of the used range according to the procedure in the previous section, and then use them for all flow rates, is probably "good enough" in many cases.

However, if greater accuracy is wanted when the flow rate varies, the variation of the injection profiles can be accounted for by the following procedure. Instead of the constants k_* and l_* in Eq. (7), they are now all set as functions of the flow, more particularly bi-variate functions of the type,

$$p(V_{inj}, f_V) \approx k(f_V)V_{inj} + l(f_V), \quad (8)$$

where f_V is the volumetric flow rate, and are used instead for each of the parameters in Eq. (7). N different flow rates $f_{V,1}$, $f_{V,2}$, …, $f_{V,N}$, (N must be at least 2) are used. For each flow rate, estimate the parameters $k(f_{V,i})$ and $l(f_{V,i})$ according to the procedure in the previous section, using at least two different experimental injection profiles. Now the function $p(V_{inj}, f_V)$ can be evaluated for the each of the flow rates $f_{V,1}$, …, $f_{V,N}$, and for any injection volume. Assume that one want to have $p(V_{inj}, f_V)$ for a flow rate $f_V \neq \{f_{V,1}, \ldots, f_{V,N}\}$, then this value can be estimated, *e.g.* by a linear least squares procedure with the data points $\{f_{V,1}, \ldots, f_{V,N}\}$, and the corresponding estimated function values $\{p(V_{inj}, f_{V,1}), \ldots, p(V_{inj}, f_{V,N})\}$.

The above procedure requires at least four experimental injection profiles: two different injection volumes at two different flow rates. In Fig. 6, this procedure was used to estimate the injection profiles for a 25.0 μL injection at four different flow rates of 0.50, 1.0 (figure inset), 2.0 and 3.0 mL/min. In the procedure four experimental injection profiles were used, with injection volumes of 50.0, 100.0, 200.0 and 400.0 μL at the flow rates 0.50 and 3.0 mL/min. In Fig. 6 (inset) the experimental and estimated injection profiles are plotted for a flow rate of 1.0 mL/min. The overlap between fitted and experimental injection profiles was 95.7, 97.2, 96.2, and 93.4% for flow rates of 0.50, 1.0, 2.0 and 3.0 mL/min, respectively. This clearly shows that the model is excellent in predicting experimental injection profiles.

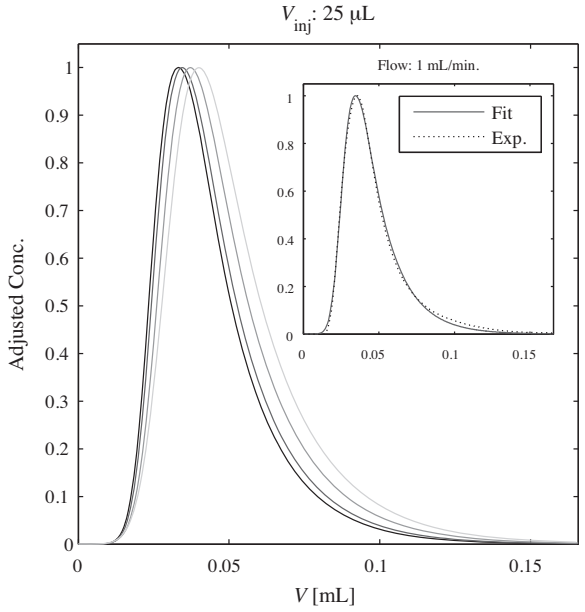

Fig. 6. Estimated flow dependence on injection profiles of 25.0 μL of a sample with concentration 1.0 mM, at the flow rates 0.50, 1.0, 2.0 and 3.0 mL/min (darker lines corresponds to lower flow rate), *cf.* Fig. 3b. All data are adjusted to a peak height of 1. The procedure in Section 4.3 was used, with experimental injection profiles with injection volumes of 50.0, 100.0, 200.0 and 400.0 μL, at the flow rates 0.50 and 3.0 mL/min. In the inset, the fitted injection profile (solid line) is shown together with experimental data (dotted line) for the flow 1.0 mL/min.

4.4. Parameter estimation by direct fit to injection profiles

It should be noted that it is possible to insert the expressions for the injection profile parameters in Eq. (7), or Eq. (8) if flow dependence is desired, into Eq. (5). This would yield a new injection profile equation with 8 parameters k_* and l_* if Eq. (7) is inserted and at least 16 parameters if Eq. (8) is inserted. All these parameters can now be estimated by fitting the new equation to experimental injection profiles. In theory just one experimental profile would now be needed, however, in a practical situation more are required.

However, this alternative approach has some drawbacks compared to the approaches suggested in Sections 4.2 and 4.3. First of all it is desirable to check that the linear relationships in Eq. (7) holds, this can easily be done with the procedure suggested in Section 4.2 but not with this alternative procedure. Secondly the non linear fitting problem is considerably harder as one now have a large number of unknown parameters that must be estimated. A more advanced algorithm that seeks the global minimum of the fitting problem must be used as the standard local search algorithm now often will yield different results depending on the starting guess of the parameters, in other words it get stuck in a local minima. These more advanced global search algorithms are not readily available and are also considerably more time consuming.

5. Conclusion

Two methods for prediction of the injection profile were examined: interpolation and a new function developed in this study. The proposed procedure in Section 4, using the new function in Eq. (5), makes it easy to get accurate estimations of the injection profiles using a very small number of experiments. To model the injection volume dependence for any injection volume, the minimum requirement is merely two experimental injection profiles, as compared to the large number required if the interpolation procedure (see Fig. 2) is used instead. This considerably simplifies accurate computer assisted process optimization, where typically the injection volume is varied in the algorithms to maximize productivity, and therefore injection profiles for any injection volume in the considered range are needed. Also, when estimating adsorption isotherm parameters using the inverse method [14] different injection volumes might be used, and the suggested procedure can hence be used to minimize the number of experimental injection profiles that needs to be measured.

The injection volume was found to be the most important parameter that needs to be accounted for in modeling of the injection profile, among the parameters usually varied in optimization of liquid chromatography. The flow rate effect on the injection profiles is usually not needed to take into account, since in most applications the flow rate is kept constant. However, if it is needed to compensate for the flow rate, this can be done by using a minimum of four experiments. The overlap between fitted and experimental injection profiles was more than 90% in all cases using experimental injection profiles from just four different injection volumes at two different flow rates.

Nomenclature

A	Gaussian peak, area
C_{exp}	experimental injection profile
C_{fit}	fitted injection profile
f	Gaussian peak function
f_V	volumetric flow rate
g	exponential decay pulse function
h	convolution between Gaussian peak function and exponential decay pulse
k_*	slope of linear fits in Eq. (7)
l_*	intercept of linear fits in Eq. (7)
p	bi-variate function, Eq. (8)
p_*	polynomial coefficients used in ln erfc function, Eq. (4)
t	time
t_0	Gaussian peak mean, time
V	eluted volume
V_0	Gaussian peak mean, eluted volume
V_{inj}	injection volume
$\bar{x}$	threshold value used in ln erfc function, Eq. (4)

Greek letters

θ	exponential decay pulse, width of constant part
σ	Gaussian peak standard deviation
τ	exponential decay pulse, decay speed of the exponential part

Acknowledgments

This work was supported in part by a grant from the Swedish Research Council (VR) for the project "Fundamental Studies on Molecular Interactions Aimed at Preparative Separations and Biospecific Measurements" and by a grant from The Research Council for Environment, Agricultural Sciences and Spatial Planning for the project "High-Value Compounds from Agricultural and Forestry Waste by Sustainable Methods – an Interdisciplinary Approach for Bioresource Utilization".

References

[1] J. Samuelsson, L. Edström, P. Forssén, T. Fornstedt, J. Chromatogr. A 1217 (2010) 4306.
[2] G. Guiochon, A. Felinger, D.G. Shirazi, A.M. Katti, Fundamentals of Preparative and Nonlinear Chromatography, 2nd ed., Elsevier Academic Press, Amsterdam, 2006.
[3] A. Felinger, G. Guiochon, J. Chromatogr. A 796 (1998) 59.
[4] A. Felinger, G. Guiochon, J. Chromatogr. A 752 (1996) 31.

[5] A. Felinger, A. Cavazzini, G. Guiochon, J. Chromatogr A 986 (2003) 207.
[6] J. Samuelsson, T. Undin, A. Törncrona, T. Fornstedt, J. Chromatogr. A 1217 (2010) 7215.
[7] J. Samuelsson, T. Fornstedt, Anal. Chem. 80 (2008) 7887.
[8] A.M. Katti, M. Czok, G. Guiochon, J. Chromatogr. 556 (1991) 205.
[9] R. Arnell, P. Forssén, T. Fornstedt, J. Chromatogr. A 1099 (2005) 167.
[10] I. Quiñones, J.C. Ford, G. Guiochon, Anal. Chem. 72 (2000) 1495.
[11] F. James, M. Sepulveda, F. Charton, I. Quinones, G. Guiochon, Chem. Eng. Sci. 54 (1999) 1677.
[12] A. Felinger, D. Zhou, G. Guiochon, J. Chromatogr. A 1005 (2003) 35.
[13] V.B. Di Marco, G.G. Bombi, J. Chromatogr. A 931 (2001) 1.
[14] P. Forssén, R. Arnell, T. Fornstedt, Comput. Chem. Eng. 30 (2006) 1381.